

Biogenic iron-containing materials synthesised in modified Lieske medium: composition, porous structure, and catalytic activity in *n*-hexane oxidation

M. Shopska*, G. Kadinov, D. Paneva, I. Yordanova, D. Kovacheva¹, A. Naydenov¹, S. Todorova, Z. Cherkezova-Zheleva, I. Mitov

Institute of Catalysis, Bulgarian Academy of Sciences, Acad. G. Bonchev St., Bldg. 11, 1113 Sofia, Bulgaria

¹*Institute of General and Inorganic Chemistry, Bulgarian Academy of Sciences, Acad. G. Bonchev St., Bldg. 11, 1113 Sofia, Bulgaria*

Received: January 26, 2018; Revised March 20, 2018

Leptothrix genus bacteria were cultivated in Lieske medium modified by the presence of inorganic material. Two modifiers were used: a fibrous 0.3% Pd/mesoporous silica-alumina catalyst and a one-side anodic oxidised aluminium foil. Obtained biomasses (named LieskeV and LieskeA, respectively) were studied by the methods of infrared and Mössbauer spectroscopy, X-ray diffraction, nitrogen adsorption, and chemical analysis. Examination of fresh samples revealed that LieskeA contained γ -FeOOH, α -FeOOH, and Fe₃O₄, whereas LieskeV comprised γ -FeOOH, α -FeOOH, and γ -Fe₂O₃ of various ratios. Elemental analysis indicated 0.003% Pd and proved that some amount of the modifier is incorporated in the LieskeV material. Registered transformations in original (biogenic or chemical) iron oxide/hydroxide phases after catalytic activity tests confirmed that LieskeV samples contained a larger amount of γ -Fe₂O₃ obtained from biogenic precursor, and some γ -FeOOH. LieskeV biomass was found to be more active in the reaction of *n*-hexane oxidation. This material also impeded incomplete oxidation to carbon monoxide. Despite very small amounts of palladium present in LieskeV samples, the latter process is probably assisted since palladium is an active catalyst for CO oxidation. Carbon monoxide oxidation in the case of LieskeV samples was stimulated by two components, which exhibit a certain activity in the studied process. Biogenic γ -Fe₂O₃ showed some intrinsic activity in CO oxidation and its dominance is a second reason for control of the incomplete hexane oxidation. A third feature of the Pd-modified samples, determining their relatively higher activity, is the presence of slightly larger pores that allow enhanced mass transfer of the reagents inside the catalytic particles.

Key words: *Leptothrix* sp., biogenic iron-containing material, hexane oxidation.

INTRODUCTION

Volatile organic compounds (VOCs) as low molecular weight hydrocarbons and oxygen containing compounds are main air pollutants. They are precursors of ozone formation in the air ground layer and have influence on processes of greenhouse gas oxidation and formation in troposphere. Volatile organic compounds together with fine dust particles cause photochemical smog formation. The smog has a harmful effect on the human health and plants. Hexane is a representative of the volatile hydrocarbons group and is widely used in a number of chemical productions as solvent or reagent, e.g. glue production, leather treatment, and pharmaceutical industry. It participates in radical reactions in the air and the formed products become involved in a photochemical smog. Hexane is included in Directive 2008/50/EC list about air quality as a compound referred to be strictly monitored and measured because it is a precursor for ozone formation [1].

One way to decrease and/or eliminate hexane emissions is their catalytic oxidation to carbon dioxide and water. The catalysts applied in this process should exhibit high activity in a wide range of reaction temperature even in the presence of various contaminants, stable performance over a large variety space velocities and substance concentrations, resistance to deactivation, and ability for regeneration [2]. There are three groups of oxidation catalysts: i) supported noble metals; ii) metal oxides and supported metal oxides; iii) mixtures of noble metal and metal oxide. The most explored catalysts for complete oxidation contain mono- and bimetallic Pt, Pd, and Rh [3,4]. They satisfy to high extent above-mentioned requirements, however, high cost and easy particle agglomeration encourage search for other active materials. Single and mixed metal oxides of Cu, Mn, Cr, Fe, and Ni can be applied as catalytic materials to this process [5,6]. Transition metal oxide catalysts are moderately resistant to sulphur poisoning and are less active at low temperatures than noble metals but a combination of several oxides could result in highly thermally stable catalysts of satisfactory activity. Transition

* To whom all correspondence should be sent
E-mail: shopska@ic.bas.bg

metal oxides of Mn, Fe, and Co are most active in the oxidation of volatile organic compounds [7]. Single metal oxides, amongst them Fe_xO_y , have also been used for this purpose [8]. It has been found that nanosized iron oxides show high activity in CO, CH_4 , C_3H_8 , and C_3H_6 oxidation, selective oxidation of alcohols and olefins, and ethylbenzene dehydrogenation [9]. They are also active in soot removal. However, published investigations on hexane oxidation in the presence of iron oxide catalysts are few.

Mixed valence oxides containing divalent and trivalent cations of transition metals form stable spinel structures of the AB_2O_4 type, in particular Fe_3O_4 . Cations with multiple oxidation states having close values of the crystal field stabilisation energy of octahedral and tetrahedral sites are the main reason for existing abundant defective spinel structures and non-stoichiometry [10]. Me_2O_3 oxides (e.g. $\gamma\text{-Fe}_2\text{O}_3$) crystallise in metastable spinel structures. Corundum is an exception because it is thermodynamically stable. Non-stoichiometric cation-deficient spinel structures are known for different transition metal oxides. These materials have been applied as oxidation catalysts and electrode materials [11–14].

Metal oxide bulk and surface oxygen mobility is significant to enhance catalyst performance in oxidation reactions. A fast electron exchange in the $\text{Fe}^{2+}/\text{Fe}^{3+}$ couple in magnetite (Fe_3O_4) is directly related to oxygen mobility that facilitates redox reactions. Iron oxide nanoparticles have largely a defect crystal structure, which is energy uncompensated. Particle sizes, smaller than about 15 nm, induce a unique magnetic property of superparamagnetism. The latter has attracted much attention because of useful applications in different fields of science and practice.

Iron oxide compounds can be synthesised by different abiotic and biotic methods. Conventional techniques (chemical, mechanical) use toxic and expensive chemicals and devices, and require high-energy consumption and detoxification of waste flows that raise catalyst costs [15–19]. However, obtained products are of good purity and have well-defined properties. Bio-inspired technologies imitate natural processes of iron mineralisation by inclusion of different mediators. One trend is to exploit different bacteria. These microorganisms are widespread in nature and their possibilities are not fully investigated and used [15,20]. Iron biomineralisation through bacteria is clean, simple, nontoxic, low-cost, and needs ambient conditions. Produced iron oxide materials are cheap. This kind of synthesis does not use dangerous reagents. Cultivation of iron bacteria for biogenic iron (oxy)(hydr)oxides synthesis takes part in diluted feeding solutions till their

nutrition components are running low or their concentration decreases under critical values related to microorganism life support. Because of that, there is no evolution of toxic products and this approach enables material preparation without evolving hazardous waste. Thus, biomineralisation methods are definitely environmentally friendly [15,18,21–30]. Ferric ion deposition by bacteria is relatively a slow process in comparison with other methods but it is not associated with energy supply because the bacteria are natural cell metabolites and no, or at least very low, energy consumption is necessary for synthesis [21–27].

Biogenic iron-containing materials are applicable to heterogeneous catalysis as catalyst precursors, active components, catalyst supports, and immobilising carriers. Studies are concentrated on different reactions and one of them is oxidation [18,19,22,28–37]. Own previously published results have shown that biogenic iron-containing materials obtained by cultivation of *Leptothrix* sp. in different feeding media exhibit a certain activity in the reaction of CO oxidation and it was found that maghemite obtained from lepidocrocite bioprecursor was more active than other bioproducts (goethite and lepidocrocite) [35]. In view of aforementioned, it is reasonable to study hexane complete oxidation in presence of biogenic iron-containing materials as a model reaction and the present work is focused on this problem.

EXPERIMENTAL

Biogenic materials were prepared by *Leptothrix* genus bacteria cultivation in Lieske medium, which contained different inorganic materials. The medium was modified by introduction of 0.3% Pd/Al-Si-O fibrous material or anodised Al foil (anodic $\text{Al}_2\text{O}_3/\text{Al}$). 0.3% Pd/Al-Si-O was obtained by sol-gel method [38], reduced at 400 °C, and then kept in air. The fibrous material was sterilised for 15 min by autoclaving at 1 atm and 120 °C. The aluminium foil was one-side covered with alumina by anodic oxidation in 0.3M $\text{H}_2\text{C}_2\text{O}_4$ electrolyte [39]. Lamellae of this material were cold sterilised by UV light. After immersing the modifiers into the feeding solutions, the latter were infected with 10% inoculum from *Leptothrix* genus bacteria. Cultivation was realised under static conditions at 20 °C for a period of 36(40) days. The produced precipitates were separated by decantation, washed with distilled water and filtered, and then dried at 40 (105) °C. The materials thus prepared are denoted as LieskeV (obtained in presence of 0.3% Pd/Al-Si-O) and LieskeA (in presence of anodic $\text{Al}_2\text{O}_3/\text{Al}$).

Powder X-ray diffraction patterns of the biogenic materials were collected within the range from 5.3

to $80^\circ 2\theta$ with a constant step of $0.02^\circ 2\theta$ on a Bruker D8 Advance diffractometer with Cu $K\alpha$ radiation and LynxEye detector. Phase identification was performed by *Diffraplus* EVA using ICDD-PDF2 Database.

Mössbauer spectra were recorded at room temperature by means of Wissenschaftliche Elektronik GmbH electromechanical apparatus (Germany), operating at a constant acceleration mode. An α -Fe standard and a $^{57}\text{Co}/\text{Rh}$ source were used. Parameters of hyperfine interactions of the obtained spectral components: isomer shift (IS), quadrupole splitting (QS), hyperfine effective field (H_{eff}), line width (FW), and component relative weight (G) were determined by CONFIT program. Computer fitting was based on the least squares method.

FTIR spectra of the materials were recorded on a Nicolet 6700 FTIR spectrometer (Thermo Electron Corporation, USA) in the far and middle IR regions. The method of dilution of studied material in a KBr pellet (0.5% of studied substance) was used. Spectra were collected using 100 scans and resolution of 4 (data spacing 1.928 cm^{-1}).

Specific surface area of both biogenic materials was measured according to the BET method (adsorption of N_2 at -196°C) by a NOVA-1200e high-speed gas sorption analyser (Quantachrome Instruments, USA). Prior to measurements, each sample was evacuated at 100°C . Pore size distribution was also estimated using the BJH method based on the isotherm desorption branch.

Catalytic measurements were carried out in an isothermal continuous flow type quartz-glass reactor (6.0 mm inner diameter) at atmospheric pressure. The catalyst was fixed in the reactor between plugs of quartz wool. Applied test conditions were: 0.63–0.8 mm catalyst fraction, 0.5 cm^3 catalyst volume, and gas hourly space velocity (GHSV) of 60.000 h^{-1} . The GHSV value was selected in order to minimise external mass transfer limitations. Reactant gases were supplied through electronic mass flow controllers. Reactant inlet concentrations were 334 ppm *n*-hexane and 20 vol.% oxygen. The gas mixture was balanced to 100% with nitrogen of 99.99% purity. Analysis of the gaseous flows was performed using a mass-spectrometer CATLAB system (Hiden Analytical, UK) by on-line gas-analysers of $\text{CO}/\text{CO}_2/\text{O}_2$ (Maihak), and a flame ionisation detector (Horiba) of the total hydrocarbon content. The studied materials were preliminary treated in the reaction flow for 30 min at 400°C in order to obtain constant composition, which would not change during the catalytic examinations.

LieskeV biogenic material elemental composition was determined on Li-tetraborate pellets using

laser ablation inductively coupled plasma-mass spectrometry. Spot analysis was done using an UP-193FX excimer laser (system) (New Wave Research Inc., USA) attached to a ELAN DRC-e quadrupole inductively coupled plasma-mass spectrometer (Perkin-Elmer Inc.). A standard reference material NIST SRM 610, a ‘squid’ smoothing device, He carrier gas, energy density on sample ca. $7.3\text{--}7.6\text{ J}\cdot\text{cm}^{-2}$, repetition rate of 10 and ablation craters $75\text{ }\mu\text{m}$ were used. The analysis was carried out in one block starting and ending with two NIST SRM 610 measurements and two measurements of the sample, which were then averaged. Two separate measurement experiments were performed in order to obtain a precise result. NIST SRM 612 was used for internal control of a possible systematic error.

RESULTS AND DISCUSSION

Elemental analysis was used to determine the amount of modifying additive, which is included in LieskeV final biogenic material. Results showed the following composition: 79.41 wt.% Fe, 8.32 wt.% Al, 9.69 wt.% Si, 0.003 wt.% Pd.

Fresh samples were studied by means of the BET method (Fig. 1). Analysis of isotherm hysteresis showed that it is of D type (or 2) [40]. This kind of hysteresis is due to heterogeneous capillaries that have large main body radii and many size-varying short necks. Pore size distribution results indicate mesoporous materials with predominant size of 4 nm. Diameters of 5–24 nm are also widely represented. Larger pores within 14–7-nm diameter are less in the case of LieskeA sample (Fig. 1B). A uniform decrease in number of pores of increasing size was found with LieskeV sample (Fig. 1B). The measured total pore volume was $0.21\text{ cm}^3/\text{g}$ for LieskeA and $0.25\text{ cm}^3/\text{g}$ for LieskeV samples. The average pore size was 11 and 10.5 nm for LieskeA and LieskeV samples, respectively. However, LieskeV biomass exposed a higher specific surface area of $95\text{ m}^2/\text{g}$ compared to $76\text{ m}^2/\text{g}$ of LieskeA counterpart.

Transmission infrared spectra of as-prepared biogenic materials (‘fresh’ samples) are shown in Fig. 2. Characteristic bands of lepidocrocite, goethite, and maghemite were recorded [25,41,42]. They are denoted γ , α , and m , respectively. Band intensity and band intensity ratios vary for the materials. Bands characteristic of feeding medium residues were also registered [43].

X-ray diffraction patterns of as-prepared samples (Fig. 3) disclose lines of the following phases: lepidocrocite (PDF01-070-8045), goethite (PDF00-029-0713), maghemite (PDF00-039-1346), and magnetite (PDF01-071-6336). Quantitative analysis results are given in Table 1.

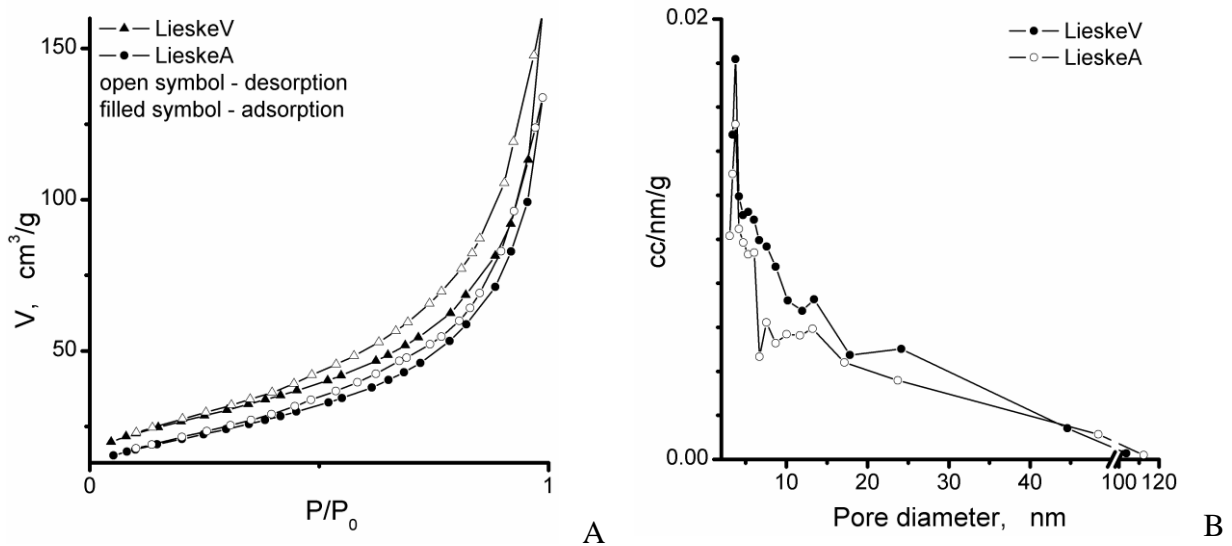


Fig. 1. Adsorption-desorption isotherms (A) and pore size distribution (B).

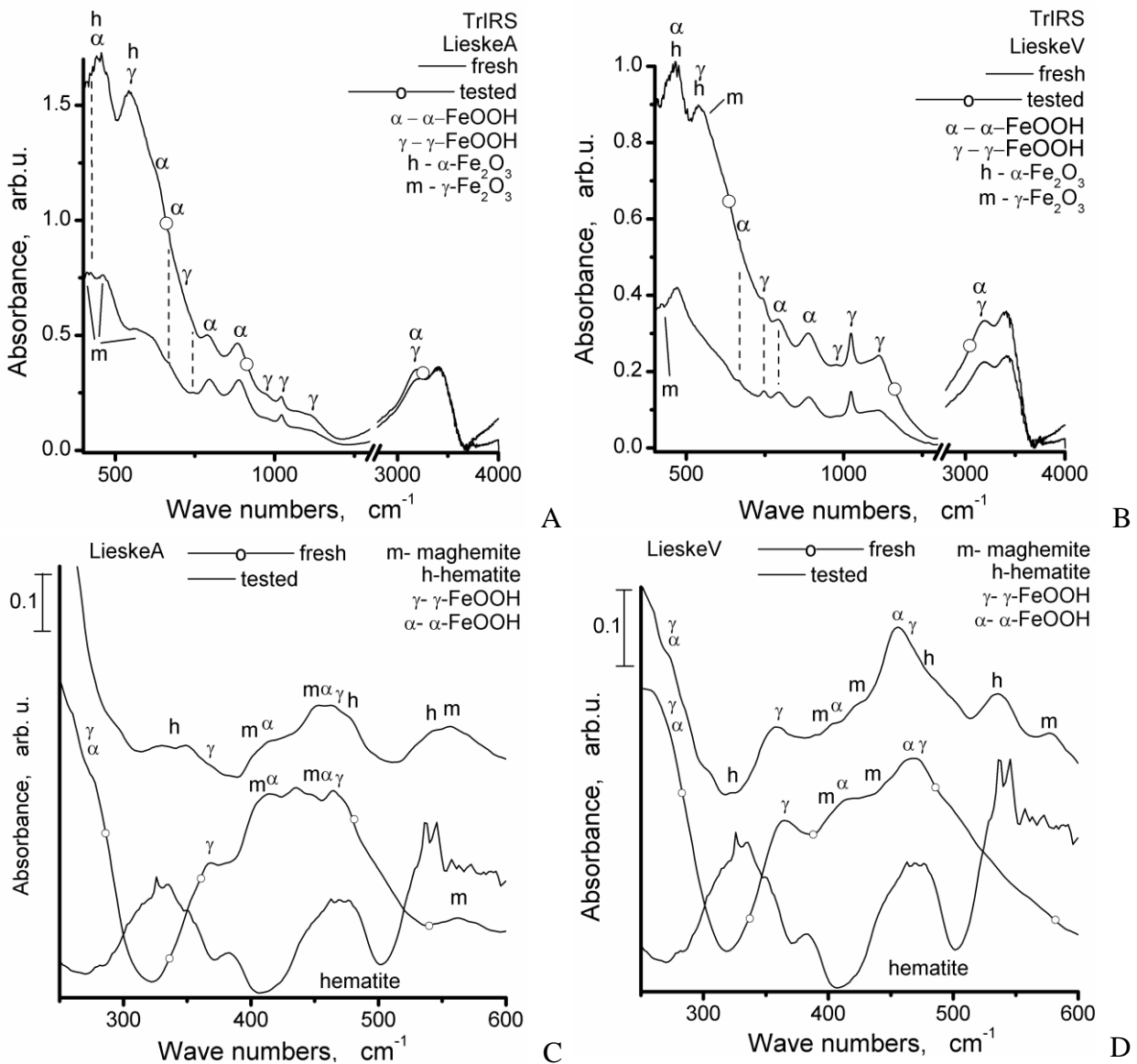


Fig. 2. IR spectra of fresh and tested samples: A, C – LieskeA, B, D – LieskeV.

Table 1. Quantitative X-ray analysis data (XRD) and Mössbauer component relative weight (G_{MS})

Component	XRD/GMS, %			
	LieskeV		LieskeA	
	fresh	tested	fresh	tested
Fe ₃ O ₄			17 / 38	
γ-Fe ₂ O ₃	7 / 7	39 / 55		23 / 53
α-Fe ₂ O ₃		36 / 21		44 / 27
α-FeOOH	60 / 17	18 / -	76 / 39	25 / -
γ-FeOOH	32 / 39	7 / 11	7 / 23	8 / 10
SPM	37	13		10

Mössbauer spectra of fresh samples were composed of doublet and sextet components and the mathematical model for calculation includes such elements. A spectrum of LieskeV sample is shown in Fig. 4A to illustrate experimental results. Isomer shift values for LieskeV samples are characteristic of octahedrally coordinated ferric ions, while in the case of LieskeA samples, Fe³⁺ ions are tetrahedrally coordinated and Fe^{2.5+} ions are positioned at octahedral sites (Table 2). Calculated parameters allow allocation of iron ions between several phases with particle sizes above 10 nm: oxyhydroxides (α-FeOOH and γ-FeOOH) and oxides (γ-Fe₂O₃ and Fe₃O₄). Some

Fe³⁺ ions in LieskeV samples are involved in oxide compounds of small particle size, below 10 nm, thus being superparamagnetic. A critical size of iron (oxy)(hydr)oxide particles that exhibit superparamagnetic properties is about 10–12 nm. In this case, the spectral components and their parameters correspond to a mixture of iron oxide compounds of two types of particles: superparamagnetic particles with sizes below 10 nm (doublets) and larger particles subjected to the model of collective magnetic excitation (CME) (sextuplets).

The biogenic materials were examined in the reaction of *n*-hexane oxidation (Fig. 5). Analyses of the reaction products showed that the process runs to CO₂ and partially to CO without any other intermediates. Analysis of the catalytic curves showed the same behaviour which is assigned to a similar reaction mechanism. The results demonstrate that LieskeV biomass is the more active material. In addition, on this type of samples, the incomplete oxidation of *n*-hexane to CO occurs to a lower extent. Despite small amount of palladium (0.003%), this modifier probably assists both processes. Palladium is well known as active catalyst for CO oxidation [44] as well for hydrocarbons oxidation [3,4].

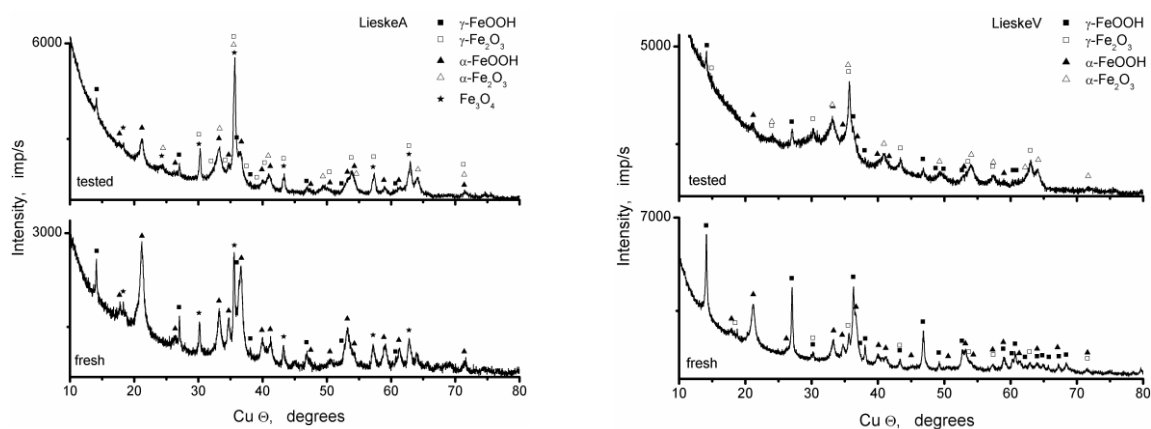


Fig. 3. X-ray diffraction patterns of fresh and tested samples.

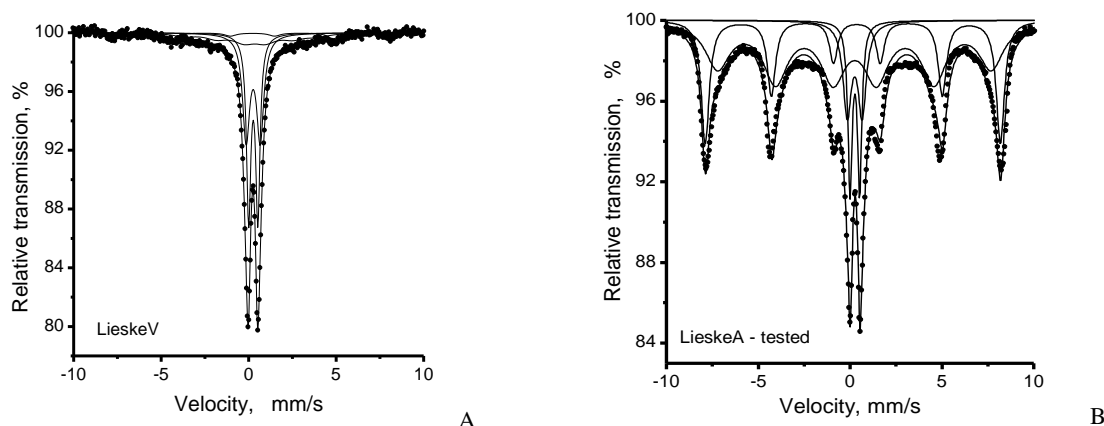


Fig. 4. Mössbauer spectra of fresh and tested samples: A – LieskeV (fresh), B – LieskeA (tested).

Table 2. Mössbauer parameters of hyperfine interaction

Sample	Components	IS, mm/s	QS, mm/s	Heff, T	FW, mm/s	G, %
LieskeV fresh	Sx1 - Fe ³⁺ _{octa} , γ -Fe ₂ O ₃	0.32	0.00	49.6	0.80	7
	Sx2 - Fe ³⁺ _{octa} , α -FeOOH	0.33	-0.12	23.5	1.50	17
	Db1 - Fe ³⁺ _{octa} , γ -FeOOH	0.36	0.53	-	0.30	39
	Db2 - Fe ³⁺ _{octa} , SPM - oxides and hydroxides	0.36	0.81	-	0.49	37
LieskeV tested	Sx1 - Fe ³⁺ _{octa} , α -Fe ₂ O ₃	0.36	-0.11	49.9	0.52	21
	Sx2 - Fe ³⁺ _{octa} , γ -Fe ₂ O ₃	0.32	0.01	45.1	1.75	55
	Db1 - Fe ³⁺ _{octa} , γ -FeOOH	0.36	0.56	-	0.31	11
	Db2 - Fe ³⁺ _{octa} , SPM - iron oxides and hydroxides	0.34	0.97	-	0.64	13
LieskeA fresh	Sx1 - Fe ³⁺ _{tetra} , Fe ₃ O ₄	0.29	0.00	49.6	0.46	17
	Sx2 - Fe ^{2.5+} _{octa} , Fe ₃ O ₄	0.64	0.00	46.4	0.90	21
	Sx3 - Fe ³⁺ _{octa} , α -FeOOH	0.33	-0.12	25.5	1.00	14
	Db1 - Fe ³⁺ _{octa} , γ -FeOOH	0.37	0.50	-	0.28	23
	Db2 - Fe ³⁺ _{octa} , α -FeOOH	0.37	0.74	-	0.46	25
LieskeA tested	Sx1 - Fe ³⁺ _{octa} , α -Fe ₂ O ₃	0.36	-0.11	50.0	0.53	27
	Sx2 - Fe ³⁺ _{octa} , γ -Fe ₂ O ₃	0.34	0.01	46.3	1.61	53
	Db1 - Fe ³⁺ _{octa} , γ -FeOOH	0.36	0.53	-	0.30	10
	Db2 - Fe ³⁺ _{octa} , SPM - iron oxides and hydroxides	0.35	0.81	-	0.54	10

Samples subjected to catalytic tests ('tested') were studied by XRD, infrared and Mössbauer spectroscopy. XRD results showed that the tested samples contain lepidocrocite (PDF01-070-8045), goethite (PDF00-029-0713), maghemite (PDF00-039-1346), and hematite (PDF01-089-0596). Quota of compounds is displayed in Table 1. Bands characteristic of lepidocrocite, goethite, maghemite, and hematite (denoted as 'h') were recorded in the infrared spectra [25,37,45]. Band intensity and band intensity ratios vary with both samples (Fig. 2, 'tested'). The Mössbauer spectra of tested and fresh samples are composed of doublet and sextet components, the second element being dominant. Spectral computation was performed following the same model. A spectrum of LieskeA sample after catalytic experiment is displayed as illustration in Fig. 4B. IS parameter values are typical of octahedrally coordinated ferric ions (Table 2). Sets of hyperfine interaction parameters are related to iron ions in α -FeOOH, γ -FeOOH, and γ -Fe₂O₃ with particle sizes above 10 nm. Fe³⁺ ions, which are included in oxide compounds with particles below 10 nm, exhibit superparamagnetic properties and amount to 10–13%. Discussion on the results obtained by the three methods revealed that most probably the superparamagnetic phase found through Mössbauer spectra analysis of tested samples is goethite. Infrared characteristic bands displayed in Fig. 2 ('tested') and diffraction lines denoted in Fig. 3 as 'tested' identify this compound. Hematite presence in the tested samples implies a transformation that has been realised during pretreatment and/or during reaction. This result is not surprising since thermal transitions of iron compounds are well-known to follow the order oxyhydroxides \rightarrow oxides

\rightarrow hematite [25,45,46].

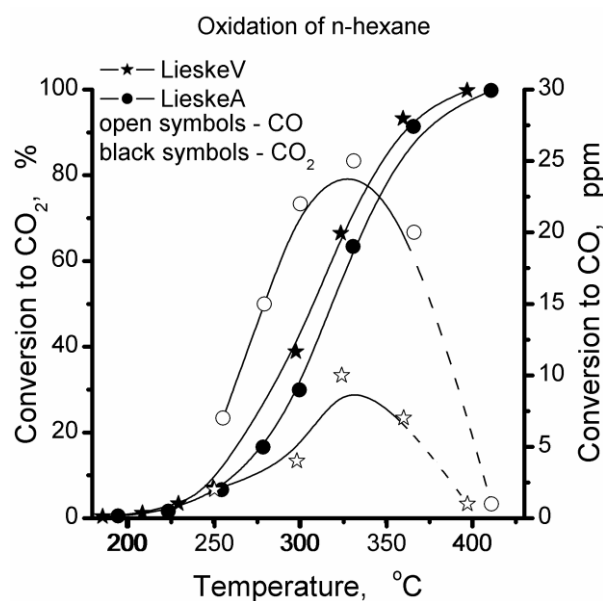


Fig. 5. Results of catalytic tests.

It is known that biomass obtained during cultivation of neutrophillic bacteria contains various iron compounds (α -FeOOH, γ -FeOOH, and β -FeOOH, and Fe_xO_y) at different ratios [41]. In addition, under selected conditions (liquid phase composition, neutral pH, and room temperature) the process of Fe²⁺ transformation to Fe³⁺ is of biogenic as well chemical nature. Iron oxides are formed in the feeding medium because of chemical reactions [47–53], however, *Leptothrix* genus participates mostly in the formation of iron oxyhydroxides [41]. Thermal conversion of goethite and lepidocrocite determines formation of biogenic maghemite.

Tested catalysts have almost the same composition, the differences being negligibly small. Bearing in mind possible transformations of iron (oxy)(hydr)oxide phases and whether they have biogenic or chemical origin [25,41,45,46], it can be affirmed that the LieskeV biomass contains a larger amount of maghemite originating from a biogenic precursor. The amount of this precursor (lepidocrocite) in fresh LieskeA biomass is less. Biogenic maghemite manifests some intrinsic activity in CO oxidation [35]. Together with available traces of palladium in LieskeV, it is reasonable to expect impeded *n*-hexane incomplete oxidation to CO. Carbon monoxide oxidation in the case of LieskeV samples is stimulated to a higher extent depending on two components that are active in this process. These special features of LieskeV biomass composition determine its higher activity at lower temperatures.

Pore structure of the studied systems has some influence on the catalytic behaviour. Although the textural features were determined for fresh samples, they could be used to explain the catalytic behaviour already discussed above. It has been found that biogenic iron is a hybrid product structured composed of iron oxide units and organic residues of bacterial origin [54-60]. It has been suggested that bacterially formed mineral deposits have wall structure, which contains iron (oxy)hydroxide spheres stabilized by organic carbon inclusions [54-57]. This structure is sterically stable to different impacts [15,28,32,34,61-63]. The LieskeV samples are characterised by relatively larger pores. This facilitates hexane molecules contact with the catalyst surface for long residence time. As a result, *n*-hexane transformation to CO₂ proceeds to a much higher extent in comparison with conversion to carbon monoxide.

CONCLUSIONS

Biogenic material, synthesised in Lieske cultivation medium in the presence of 0.3% Pd/Al-Si-O fibrous catalyst, was more active in the reaction of *n*-hexane oxidation than a counterpart material synthesised in the same medium in the presence of anodic oxidised aluminium foil. Incomplete oxidation to CO was also registered, however, to a lower extent if compared with the latter biomass. Beneficial catalytic properties were determined by two basic factors: (i) presence of traces of the 0.3% Pd/Al-Si-O fibrous material, which actually corresponds to 0.0003% Pd in the biomass and (ii) larger amount of maghemite obtained from a biogenic precursor in comparison with the material formed in presence of alumina/Al lamellae. Contribution by relatively larger pores and higher specific surface area is also suggested.

Acknowledgements: The authors are grateful to Bulgarian Science Fund for financial support by project T02-17/2014. Preparation of the anodic alumina/Al support by Assoc. Prof. B. Tsaneva from Technical University, Sofia, and of the biogenic materials by Prof. V. Groudeva and co-workers from Faculty of Biology of St. Kliment Ohridski University of Sofia is greatly acknowledged.

REFERENCES

1. Directive 2008/50/EC of the European Parliament and of the Council of 21 May 2008 on ambient air quality and cleaner air for Europe, *Official Journal of the European Union*, **L 152**, 1-44 (11.6.2008).
2. R.M Heck, R.J. Farrauto, *Catalytic Pollution Control*, second ed., Wiley-Interscience, New York, 2002.
3. S. C. Kim, W. G. Shim, *Appl. Catal. B: Environ.*, **92**, 429 (2009).
4. L. F. Liotta, *Appl. Catal. B: Environ.*, **100**, 403 (2010).
5. K. Everaert, J. Baeyens, *J. Hazard. Mater.*, **109**, 113 (2004).
6. J. J. Spivey, *Ind. Eng. Chem. Res.*, **26**, 2165 (1987).
7. U. Zavyalova, P. Scholz, B. Ondruschka, *Appl. Catal. A: General*, **323**, 226 (2007).
8. S. Scirè, S. Minicò, C. Crisafulli, S. Galvagno, *Catal. Commun.*, **2**, 229 (2001).
9. M. Baldi, V. S. Escribano, J. M. G. Amores, F. Milella, G. Busca, *Appl. Catal. B-Environ.*, **17**, L175 (1998).
10. A. Wells, *Structural Inorganic Chemistry*, 5th ed., Clarendon Press, Oxford, 1986, Ch. 13.
11. H. Hung, *Stud. Surf. Sci. Catal.*, **45**, 171 (1989).
12. J. Barrault, C. Renard, *Appl. Catal.*, **14**, 133 (1985).
13. T. Baird, K. Campbell, P. Holliman, R. Hoyle, D. Stirling, B. Williams, M. Morris, *J. Mater. Chem.*, **7**, 319 (1997).
14. A. C. Tavares, M. A. Cartaxo, M. I. Pereira, F. M. Costa, *J. Electroanal. Chem.*, **464**, 187 (1999).
15. A. B. Seabra, P. Haddad, N. Duran, *IET Nanobiotechnol.*, **7**, 90 (2013).
16. K. B. Narayanan, N. Sakthivel, *Adv. Coll. Interface Sci.*, **156**, 1 (2010).
17. H. Jung, J.-W. Kim, H. Choi, J.-H. Lee, H.-G. Hur, *Appl. Catal. B: Environ.*, **83**, 208 (2008).
18. B. Kazprzyk-Hordern, M. Ziolek, J. Nawrocik, *Appl. Catal. B: Environ.*, **46**, 639 (2003).
19. T. Shahwan, S. Abu Sirriah, M. Nairat, E. Boyaci, A. E. Eroglu, T. B. Scott, K. R. Hallam, *Chem. Eng. J.*, **172**, 258 (2011).
20. T. Ema, Y. Miyazaki, I. Kozuki, T. Sakai, H. Hashimoto, J. Takada, *Green Chem.*, **13**, 3187 (2011).
21. H. Hashimoto, S. Yokoyama, H. Asaoka, Y. Kusano, Y. Ikeda, M. Seno, J. Takada, T. Fujii, M. Nakanishi, R. Murakami, *J. Magnet. Magnet. Mater.*, **310**, 2405 (2007).
22. T. Sakai, Y. Miyazaki, A. Murakami, N. Sakamoto, T. Ema, H. Hashimoto, M. Furutani, M. Nakanishi, T. Fujiia, J. Takada, *Org. Biomol.Chem.*, **8**, 336 (2010).

23. B. Xin, D. Zhang, X. Zhang, Y. Xia, F. Wu, S. Chen, L. Li, *Bioresour. Technol.*, **100**, 6163 (2009).
24. J. A. Rentz, I. P. Turner, J. L. Ullman, *Water Res.*, **43**, 2029 (2009).
25. R. Cornell, U. Schwertmann, *Iron Oxides*, Wiley-VCH Verlag, Weinheim, Germany, 2003.
26. R. W. Fitzpatrick, R. Naidu, P. G. Self, in: *Biomine-ralization Processes of Iron and Manganese - Modern and Ancient Environments*, Catena Supplement 21, H. C. W. Skinner, R. W. Fitzpatrick (eds.), Catena Verlag, Reiskirchen, Germany, 1992, p. 263.
27. D. A. Ankrah, E. G. Sogaard, in: *13th Int. Water Technol. Conf.*, IWTC 13, Hurgada, Egypt, 2009, p. 999.
28. T. Ema, Y. Miyazaki, I. Kozuki, T. Sakai, H. Hashimoto, J. Takada, *Green Chem.*, **13**, 3187 (2011).
29. A. Alharthi, R. A. Blackley, T. H. Flowers, J. S. J. Hergreaves, I. D. Pulford, J. Wigzell, W. Zhou, *J. Chem. Technol. Biotechnol.*, **89**, 1317 (2014).
30. G. E. Hoag, J. B. Collins, J. L. Holcomb, J. R. Hoag, M. N. Nadagouda, R. S. Varma, *J. Mater. Chem.*, **19**, 8671 (2009).
31. H. Jung, H. Park, J. Kim, J.-H. Lee, H.-G. Hur, N. V. Myung, H. Choi, *Environ. Sci. Technol.*, **41**, 4741 (2007).
32. K. Mandai, T. Korenaga, T. Ema, T. Sakai, M. Furutani, H. Hashimoto, J. Takada, *Tetrahedron Lett.*, **53**, 329 (2012).
33. R. A. Maithreepala, R.-A. Doong, *Chemosphere*, **70**, 1405 (2008).
34. B. Kumar, K. Smita, L. Cumbal, A. Debut, *J. Saudi Chem. Soc.*, **18**, 364 (2014).
35. M. Shopska, D. Paneva, G. Kadinov, S. Todorova, M. Fabian, I. Yordanova, Z. Cherkezova-Zheleva, I. Mitov, *React. Kinet. Mech. Catal.*, **118**, 179 (2016).
36. M. Shopska, Z. Cherkezova-Zheleva, D. Paneva, M. Iliev, G. Kadinov, I. Mitov, V. Groudeva, *Cent. Eur. J. Chem. (Open Chemistry)*, **11**, 215 (2013).
37. M. G. Shopska, D. G. Paneva, H. G. Kolev, G. B. Kadinov, R. Ilieva, M. Iliev, Z. P. Cherkezova-Zheleva, I. G. Mitov, *Helv. Chim. Acta*, **100**, e1700172 (2017).
38. L. Spasov, P. Dimitrov, Ch. Vladov, V. Zhelyazkov, Ch. Bonev, L. Petrov, in: *Heterogeneous Catalysis (Proc. 8th Int. Symp. Heterogen. Catal., Varna, 5–9 October 1996)*, Institute of Catalysis, Bulgarian Academy of Sciences, Sofia, 1996, p. 751.
39. B. R. Tzaneva, A. I. Naydenov, S. Zh. Todorova, V. H. Videkov, V. S. Milusheva, P. K. Stefanov, *Electrochim. Acta*, **191**, 192 (2016).
40. A. Adamson, *Physical Chemistry of Surfaces*, 3rd ed., Z. M. Zorin, V. M. Muller (eds.), Mir, Moscow, 1979.
41. M. Shopska, D. Paneva, G. Kadinov, Z. Cherkezova-Zheleva, I. Mitov, M. Iliev, *Appl. Biochem. Biotechnol.*, **181**, 867 (2017).
42. B. Weckler, H. D. Lutz, *Eur. J. Solid State Inorg. Chem.*, **35**, 531 (1998).
43. L. H. Little, *Infrared spectra of adsorbed species*, Academic Press Inc., London, New York, 1966.
44. O. V. Krylov, *Heterogeneous Catalysis: Textbook*, Akademkniga, Moscow, 2004.
45. H. Lepp, *Am. Miner. (Notes and News)*, **42**, 679 (1957).
46. A. U. Gehring, A. M. Hofmeister, *Clays Clay Miner.*, **42**, 409 (1994).
47. H. L. Ehrlich, D. K. Newman, *Geomicrobiology*, USA: CRC Press - Taylor & Francis Group, 2009.
48. A. Kappler, K. L. Straub, *Geomicrobiological Cycling of Iron*, In: *Molecular Geomicrobiology* (J. F. Banfield, J. Cervini-Silva, K. H. Nealson, Eds.), *Reviews in Mineralogy and Geochemistry*, vol. 59 (J. J. Rosso, Series ed.), Mineralogical Society of America (Geochemical Society), 2005.
49. M. Shopska, S. Todorova, I. Yordanova, S. Mondal, G. Kadinov, *Bulg. Chem. Commun.*, **47** (Special issue C), 73 (2015).
50. D. Emerson, J. V. Weiss, *Geomicrobiol. J.*, **21**, 405 (2004).
51. S. Vollrath, T. Behrends, C. Bender Koch, P. Van Cappellen, *Geochim. Cosmochim. Acta*, **108**, 107 (2013).
52. E. D. Melton, E. D. Swanner, S. Behrens, C. Schmidt, A. Kappler, *Nature Reviews. Microbiology*, **12**, 797 (2014).
53. Z. Cherkezova-Zheleva, M. Shopska, D. Paneva, D. Kovacheva, G. Kadinov, I. Mitov, *Hyperfine Interact.*, **237**, (2016).
54. C. S. Chan, S. C. Fakra, D. S. Edwards, D. Emerson, J. F. Banfield, *Geochim. Cosmochim. Acta*, **73**, 3807 (2009).
55. F. G. Ferris, R. O. Hallberg, B. Lyven, K. Pedersen, *Appl. Geochem.*, **15**, 1035 (2000).
56. K. Benzerara, T. H. Yooch, T. Tyliczszak, B. Constantz, A. M. Spormann, G. E. Brown, Jr., *Geobiology*, **2**, 249 (2004).
57. D. Emerson, H. Lin, L. Agulto, L. Lin, *Bioscience*, **58**, 925 (2008).
58. T. Suzuki, H. Hashimoto, H. Ishihara, T. Kasai, H. Kunoh, J. Takada, *Appl. Environ. Microbiol.*, **77**, 7873 (2011).
59. M. Furutani, T. Suzuki, H. Ishihara, H. Hashimoto, H. Kunoh, J. Takada, *Minerals*, **1**, 157 (2011).
60. M. G. Shopska, Z. P. Cherkezova-Zheleva, D. G. Paneva, V. Petkova, G. B. Kadinov, I. G. Mitov, *Croat. Chem. Acta*, **87**, 161 (2014).
61. T. Shahwan, S. Abu Sirriah, M. Nairat, E. Boyaci, A. E. Eroglu, T. B. Scott, K. R. Hallam, *Chem. Eng. J.*, **172**, 258 (2011).
62. M. Harshiny, C. N. Iswarya, M. Matheswaran, *Powder Technol.*, **286**, 744 (2015).
63. T. Ema, Y. Miyazaki, T. Taniguchi, J. Takada, *Green Chem.*, **15**, 2485 (2013).

БИОГЕННИ ЖЕЛЯЗО-СЪДЪРЖАЩИ МАТЕРИАЛИ СИНТЕЗИРАНИ В МОДИФИЦИРАНА СРЕДА НА ЛИСКЕ – СЪСТАВ, ПОРИСТА СТРУКТУРА И КАТАЛИТИЧНА АКТИВНОСТ В ОКИСЛЕНИЕТО НА *n*-HEКСАН

М. Шопска*, Г. Кадинов, Д. Панева, Ил. Йорданова, Д. Ковачева¹, Ант. Найденов¹, С. Тодорова, З. Черкезова-Желева, Ив. Митов

Институт по катализ, Българска академия на науките, ул. „Акад. Г. Бончев“ бл. 11, 1113 София, България

¹ Институт по обща и неорганична химия, Българска академия на науките, ул. „Акад. Г. Бончев“ бл. 11, 1113 София, България

Постъпила на 26 януари 2018 г.; Преработена на 20 март 2018 г.

(Резюме)

Бактерии от род *Leptothrix* са култивирани в среда на Лиске модифицирана с неорганичен материал. Използвани са два вида модификатори: 0.3% Pd/мезопорест Al-Si-O влакнест катализатор и едностранно анодно окислено алуминиево фолио. Получените биомаси (означени съответно ЛискеВ и ЛискеА) са изследвани чрез методите инфрачервена и Мьосбауерова спектроскопия, Рентгенова дифракция, адсорбция на азот и каталитични изпитания. Охарактеризирането на свежи образци показва, че ЛискеА съдържа γ -FeOOH, α -FeOOH и Fe₃O₄, докато ЛискеВ се състои от γ -FeOOH, α -FeOOH и γ -Fe₂O₃ в различни съотношения. Чрез елементарен анализ бе доказано, че малко количество от модифициращия материал е включено в ЛискеВ и образецът съдържа 0.003% Pd. Регистрирани превръщания на изходните (биогенни и абиотични) желязооксидни/хидроксидни фази след участието на материалите в каталитичните изпитания потвърдиха, че образец ЛискеВ съдържа по-голямо количество γ -Fe₂O₃, получен от биогенен прекурсор, както и малко количество γ -FeOOH. Беше установено, че материалът ЛискеВ е по-активен в реакцията на окисление на *n*-хексан. Освен това, в присъствие на този образец непълното окисление до СО протича в по-малка степен. Въпреки, че паладият присъства в много малко количество в образец ЛискеВ, той най-вероятно подпомага каталитичния процес, тъй като е активен катализатор за окислението на СО. При употребата на образец ЛискеВ окислението на СО се стимулира от два компонента, които са активни в изследвания процес. Активност в окислението на СО е присъща и на биогенния γ -Fe₂O₃, а по-високото му съдържание в образца е втората причина за по-ниската степен на непълно окисление на C₆H₁₄. Трета особеност на образец ЛискеВ, която определя неговата относително по-добра активност, е присъствието на малко по-широки пори, което позволява подобрен масопренос на реагентите в катализаторните частици.